THE DYNAMIC APERTURE OF LEP AT HIGH ENERGY

J.M. Jowett, Y. Alexahin*, F. Ruggiero, S. Tredwell†,
CERN, Geneva, Switzerland

Abstract

At the highest operating energies of LEP, the beam occupies a large phase space volume (emittances) because of the strong synchrotron radiation effects. The stable phase space volume required is comparable to the dynamic aperture, itself in large part determined by radiative effects such as beta-synchrotron coupling. Tune-dependences on the three oscillation amplitudes are also important. We review the present understanding of the physics of the dynamic aperture, the computational techniques used to evaluate it and their relation to the most recent measurements. Improvements in dynamic aperture can be achieved by a variety of means including changes of optics, tunes, multipole correctors and the RF voltage distribution.

1 INTRODUCTION

To a greater extent than in previous e^+e^- rings, single particle dynamics in LEP2 (beam energies from 80 to 96 GeV) will be governed by the large synchrotron radiation loss (about 2 % per turn) and associated effects of "energy-sawtoothing", radiation damping and quantum excitation [2], coupled with the non-linear dynamics due to sextupoles and other elements.

The layout, parameters and optics of LEP2 are described in more detail elsewhere [8]; we mention the high values of the synchrotron tune $Q_s \simeq$ 0.1-0.15 needed to maintain adequate quantum lifetime at high energy.

To maximise luminosity it is preferable to use a lower emittance optics than at LEP1 (45.6 GeV) where phase advances were $(\mu_x, \mu_y) = (90°, 60°)$ in the arc cells. Present plans are to operate LEP2 with an optics with $(\mu_x, \mu_y) = (108°, 60°)$. In each arc there are 2 horizontally focusing and 3 vertically focusing families of sextupoles.

We refer to [2] and references therein for the equations of motion with radiation. Particle coordinates are expressed in terms of primitive canonical variables $(x, p_x, y, p_y, t, p_t))$ with respect to a reference trajectory (all coordinates in units of length and all momentums in units of the reference p_0). Once the 6-dimensional closed orbit is found the motion can be expressed in terms of the normal modes of linear oscillation around it. By convention, we represent dynamic apertures in terms of amplitude variables related to the normal mode actions by $(A_x, A_y, A_t) = (2I_1, 2I_2, 2\gamma_{p_t} I_3)$ and the three conjugate phase variables (ϕ_x, ϕ_y, ϕ_t). Suffixes reflect the *dominant component* of each normal mode. The factor γ_{p_t} is such that averages over the beam distribution give the emittances $\langle A_{x.y}/2\rangle = \epsilon_{x,y}$ and fractional energy spread $\langle A_t/2\rangle = \sigma_\epsilon^2$.

* Visitor from PPL JINR, Russia

† Technical Student from University of Bath, UK

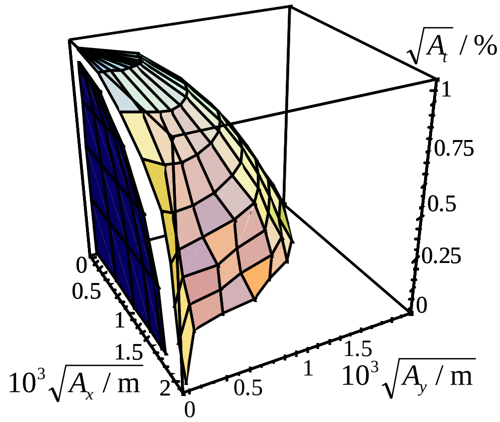

Figure 1: Dynamic aperture of the $(108°, 60°)$ optics with the RF configuration (total voltage $V_{\mathrm{RF}} = 1898$ MV foreseen for operation at 87 GeV later in 1996. The flat inner surface is a notional beam-stay-clear corresponding to 10, 10 and 7 "sigmas" of the normal modes.

2 COMPUTING DYNAMIC APERTURE

Numerical tracking is, as usual, our main tool for calculating the dynamic aperture of LEP. Our tracking engine, the program MAD [6], includes a faithful, element-by-element, photon-by-photon representation of the synchrotron radiation [2]. All non-linear quantum excitation and radiation damping effects are generated naturally.

We usually track with (deterministic) radiation damping [2]. Around 90 GeV, 50–100 turns of the ring are sufficient to determine unambiguously whether a particle is stable. Nevertheless, a full 6-dimensional scan of the initial conditions $(A_x, A_y, A_t, \phi_x, \phi_y, \phi_t)$ is expensive in computer time. However 4-dimensional scans of (A_x, A_y, A_t, ϕ_t) (with fixed initial $\phi_x = \phi_y = 0$) are *essential* for LEP.

Tracking technology We have developed a package [5] (written in the Mathematica programming language in object-oriented style) to automate the evaluation and facil-

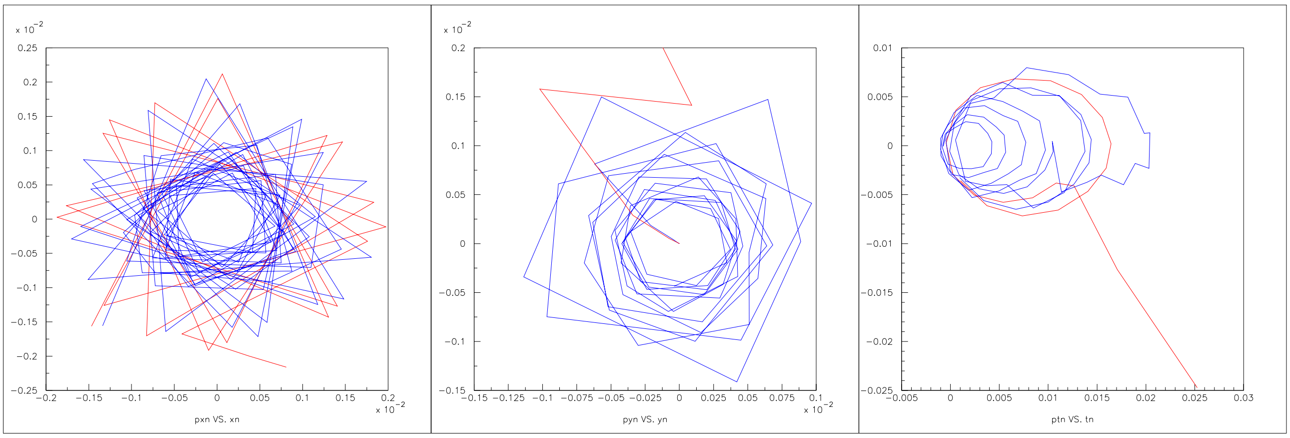

Figure 2: [Stability limit for the horizontal mode seen in the phase planes of the three normal modes of linear oscillation around the closed orbit. Two particles are started with $A_y = A_t =$ and with values of A_x just inside (blue) and outside (red) the dynamic aperture. In both cases, resonant growth soon occurs in the (y_n, p_{yn})-plane. RBSC generates "synchrotron oscillations" about an oscillation centre that damps back towards the stable phase of the closed orbit $t_n = 0$. The additional radiation loss from the larger initial A_x is enough to make the particle unstable. The growth also triggers a vertical betatron instability because Q_y has shifted with the increase of A_x.

itate the subsequent display and analysis of dynamic apertures. The laborious process of running MAD iteratively to construct the boundary surface of the dynamic aperture is efficiently handled by the evaluation of a single function **`findDynap`** whose arguments specify the scope (e.g., range of polar angles in (A_x, A_y, A_t) space), precision and confidence required of the scan. The user is completely relieved from perusing MAD's output. Typical scans for LEP involve tracking 700–4000 particles.

The tracking process creates two kinds of data-objects. Their properties and methods are implemented as overloaded functions using Mathematica's pattern-matching capabilities. These functions are easy to use interactively to display and analyse the results.

`survivalData` objects contain full information about the survival times of particles. They can be transformed into **`dynapData`** objects which represent the dynamic aperture surface. The properties of these objects include attributes such as beam emittances, tunes and other descriptive information. Their methods include a variety of 2-D and 3-D dynamic aperture and survival plots, tabulations, data-merges and so on. The internal structure of the objects is easily extended and new functions are easily written to add capabilities to the package.

Figure 1 is an example for a current optics.

3 DYNAMIC APERTURE LIMITS

Although there are many ways in which particles can become unstable, some characteristic phenomena can be identified in the three extremities of Figure 1.

The maximum stable synchrotron amplitude A_t is a consequence of the finite RF voltage. Chromatic effects become more important if V_{RF} is increased.

The limitation in A_y arises from the Radiative Beta-Synchrotron Coupling (RBSC) instability [2]. Increasing the focusing at the collision point (reducing β_y^* or β_x^*) may enhance this instability via the increased radiation loss at large betatron amplitudes in the quadrupoles of the interaction region.

The most serious limitation is in A_x. It arises from the combination of tune-dependence on amplitude and RBSC as illustrated by the example in Figure 2. The $(108^\circ, 60^\circ)$ optics has a large value of $\frac{\partial Q_y}{\partial A_x}$ [1] which leads to vertical betatron instability.

The value of $\frac{\partial Q_y}{\partial A_x}$ is much smaller in a $(108^\circ, 90^\circ)$ optics [1], leading naturally to a proposal to switch to such an optics in order to reach the highest energies. A prototype was tested experimentally in 1995 (see below). The limit in A_x is then given purely by RBSC but is more sensitive to imperfections. This is a more effective way to increase the dynamic aperture than others such as additional sextupole and octupole correctors [1] and changes of the tunes.

4 MEASUREMENTS

We report on measurements of low-emittance optics at 45.6 and 65 GeV. LEP will reach higher energies later this year.

Most often, we use a pulsed injection kicker to excite horizontal oscillations of a bunch, increasing the amplitude until a partial or total loss occurs. The analysis of single-kick measurements is simple for a kicker voltage corresponding to a bunch current loss of 50%, the dynamic aperture is $\sqrt{A_x} = \sqrt{\beta_x^{\mathrm{kick}}}\Delta p_x$.

The horizontal aperture was first measured for a positron beam on the $(108^\circ, 60^\circ)$ optics at 45.6 GeV with $\beta_y^* = 5\,\mathrm{cm}$ [9]. With damping and emittance wigglers at maximum, the measured emittances were $\epsilon_x = 20\,\mathrm{nm}$, $\epsilon_y = 1\,\mathrm{nm}$.

The measured dynamic aperture for positrons $\sqrt{A_x^+} =$

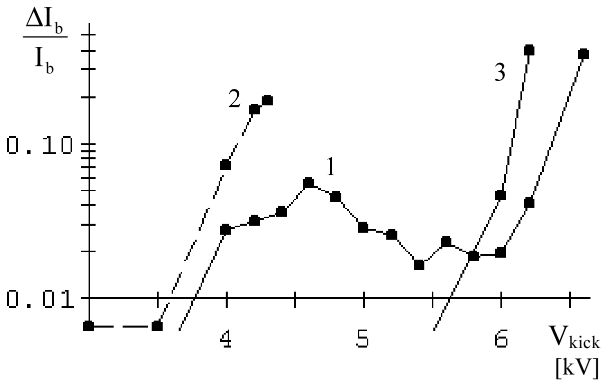

Figure 3: Relative bunch current loss vs. kicker voltage under different conditions for the $(108°, 90°)$ optics at 45.6 GeV (from [1]): 1) $\beta_y^* = 9$ cm and no wigglers, 2) $\beta_y^* = 9$ cm and emittance plus damping wigglers switched on, 3) $\beta_y^* = 5$ cm and no wigglers.

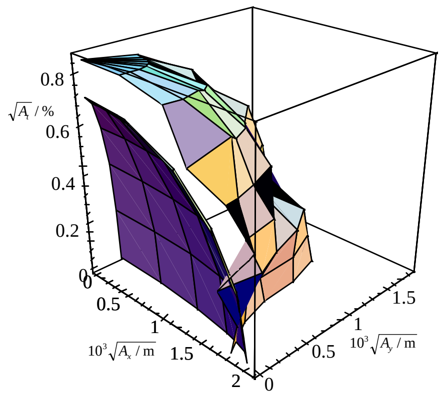

Figure 4: Calculated dynamic aperture for experimental conditions on the $(108°, 60°)$ optics 65 GeV ($V_{\mathbf{RF}} = 601$ MV): beam ellipsoid for $\epsilon_x = 39$ nm and $\epsilon_y = 0.5$ nm.

$1.0 \times 10^{-3}\sqrt{\mathrm{m}}$ is considerably smaller than the value obtained by tracking (without wigglers), namely $\sqrt{A_x} = 1.65 \times 10^{-3}\sqrt{\mathrm{m}}$ but the discrepancy may be a consequence of a kicker timing error. For electrons in the same conditions, the result was $\sqrt{A_x} = 1.5 \times 10^{-3}\sqrt{\mathrm{m}}$ in fairly close agreement with tracking predictions.

In tests of an experimental $(108°, 90°)$ optics at 45.6 GeV [1], an electron beam was kicked in various conditions. Figure 3 shows the resulting bunch current losses.

In cases 1 and 3, the kicker voltages of 6.6 kV and 6.2 kV correspond to a dynamic aperture of $\sqrt{A_x} = (2.2\text{–}2.4) \times 10^{-3}\sqrt{\mathrm{m}}$, in agreement at the 10% level with the calculated $\sqrt{A_x} = 2.5 \times 10^{-3}\sqrt{\mathrm{m}}$. In case 2, significant losses appeared at a kicker voltage around 4.2 kV (see curve 2 in Figure 3): the corresponding emittance and relative energy spread were $\epsilon_x = 24$ nm and $\sigma_\epsilon = 1.4 \times 10^{-3}$, respectively. With wigglers on and $\beta_y^* = 5$ cm, the electron beam had a poor lifetime because the sextupole family structure was inappropriate for this optics.

The structure of the losses in case 1 has been associated with an imperfection-driven third order resonance. For a certain kick, particles are trapped and subsequently escape to larger amplitudes via quantum fluctuations [1].

Measurements at 65 GeV on the $(108°, 60°)$ optics [10] were done by increasing the horizontal emittance using the wigglers and then reducing the horizontal damping rate by a reduction of the RF frequency. For e^+ with $\beta_y^* = 5$ cm and emittance wigglers at maximum, the calculated/measured emittance was $\epsilon_x = 31/35$ nm. Then the RF frequency was reduced by 50 Hz, corresponding to a partition number $J_x = 0.76$ and emittance $\epsilon_x = 39/45$ nm with good lifetime. The vertical emittance remained around $\epsilon_y = 0.5$ nm. A further reduction of the RF frequency by 50 Hz led to an emittance $\epsilon_x = 60/62$ nm and poor beam lifetime.

The calculation corresponding to experimental conditions after the first 50 Hz reduction of RF frequency is shown in Fig. 4: the available dynamic aperture is too small to accommodate the nominal $(10, 10, 7)\,\sigma$ beam ellipsoid.

However, a *single* beam has a good lifetime provided the available aperture is about 7 σ in all three planes (the 10 σ criterion is intended for beams in collision). The dynamic aperture in Fig. 4 is about $8\sigma_x$ for a beam with $\epsilon_x = 60\,\mathrm{nm}$. We conclude that the experiment at 65 GeV is quite compatible with predictions.

5 CONCLUSIONS

Although the physics determining the dynamic aperture of LEP is quite different from other machines, computation and measurement agree rather well. Forthcoming experiments will help to settle the question of how much dynamic aperture is needed and the best choice of optics.

Acknowledgements: Over the past 15 years, colleagues too numerous to mention have contributed to the understanding of LEP's dynamic aperture.

6 REFERENCES

[1] Y. Alexahin, CERN–SL–95–110 (AP) 1995.

[2] F. Barbarin, F.C. Iselin, and J.M. Jowett, Proc. 4th European Particle Accelerator Conf., World Scientific, Singapore, 1994, p. 193.

[3] J.M. Jowett, in Proc. 4th Workshop on LEP Performance, CERN SL/94-06 (DI) (1994).

[4] J. Liu et al., Proc. 1993 Particle Accelerator Conf., p. 285.

[5] J.M. Jowett, S. Tredwell, CERN SL Report, to appear, 1996.

[6] H. Grote, F.C. Iselin, CERN SL 90–13 (AP) rev. 5 (1996).

[7] F. Ruggiero, in Proc. 4th and 5th Workshops on LEP Performance, CERN SL/94-06 (DI) 73 (1994) and CERN SL/95-08 (DI) 164 (1995).

[8] LEP2 Design Report, CERN report to appear, 1996.

[9] D. Brandt et al, CERN SL-MD Note 189 (1995).

[10] C. Arimatea et al, CERN SL-MD Note 199 (1995).